Shear behaviour of rammed earth walls repaired by means of grouting

SILVA, R.A.[1]; OLIVEIRA, D.V.[2]; SCHUEREMANS, L.[3]; MIRANDA, T.[4]; MACHADO, J.[5]

ABSTRACT: Southern Portugal presents a rich heritage constituted by several constructions made from unstabilised rammed earth (URE), which are threatened by several factors, ranging from lack of conservation to a non-negligible seismic hazard. These threatens are enhanced by the fact that little is known about the shear behaviour of URE constructions. The preservation of this heritage requires definitely the development of this knowledge and, in addition, the development of adequate intervention solutions. This paper presents an experimental program where the shear behaviour of URE is assessed by means of diagonal compression tests on representative wallet-specimens. Furthermore, the use of mud grouts in repairing cracks was also assessed. The results showed that the shear behaviour of URE depends on the binding capacity promoted by the clay fraction and on the friction and interlocking promoted by the coarse aggregates. The repair by injection was shown to promote satisfactory shear strength recovery of the specimens, but was less effective in recovering the initial shear stiffness.

Keywords: Rammed earth, shear-behaviour, repair, injection, mud grout

1 INTRODUCTION

Earth constructions are frequently associated to vernacular architecture, since they are frequently built by local communities using local materials. From this intrinsic diversity resulted several known building techniques, but the most common and widespread are the adobe masonry and rammed earth [1-2]. These techniques are used since ancient times to build from simple dwellings to monuments and military constructions. Nowadays, the population in many developing countries, such as Peru, India and Yemen, use intensively these techniques as low cost housing solutions. Furthermore, it is estimated that about one fourth of the World's population still lives in an earth building [3]. As a consequence, a large housing stock built from earth exists widely distributed around the world [1]. Furthermore, some sites and buildings among this heritage feature an important historical, cultural and architectonical value, which is important to preserve. The Great Wall of China is a great example of such important heritage, where many of its sections were built in rammed earth [4].

Rammed earth, also known as "*taipa*", "*taipa de pilão*" "*tapial*", "*pise de terre*", "*pisé*" or "*stampflehm*", consists in compacting moist earth by layers inside a removable formwork to build monolithic walls (see Figure 1). In fact, the formwork constitutes a key feature that differentiates this technique from others. The conception and design of the formwork have suffered an evolving process, which resulted in several configurations. The construction of a traditional wall is carried out by courses (like masonry), where the formwork runs horizontally along the perimeter of the construction and then is

[1] PhD, ISISE, Department of Civil Engineering, ruisilva@civil.uminho.pt
[2] PhD, ISISE, Department of Civil Engineering, danvco@civil.uminho.pt
[3] PhD, Frisomat/KULeuven, Department of Civil Engineering, luc.schueremans@bwk.kuleuven.be
[4] PhD, ISISE, Department of Civil Engineering, tmiranda@civil.uminho.pt
[5] MSc student, University of Minho, Department of Civil Engineering, juliocmachado.85@gmail.com

lifted to build the next course. Nowadays, the trend is to use the same metallic shutters used in concrete technology to constitute a formwork that covers the entire wall. The compaction of a rammed earth wall can be executed resorting to manual rammers (made of timber) or to pneumatic and vibratory rammers, which allow reducing substantially the labour and time consumed in the construction. The dimensions of the rammed earth blocks from traditional dwellings are very variable from region to region. For example, in Alentejo (Portugal) the length of rammed earth blocks from typical dwellings may vary from 1.40 m to 2.50 m, the height from 0.4 m to 0.55 m and the thickness from 0.4 m to 0.57 m [9].

Figure 1. Rammed earth house being built in Odemira, Portugal.

The rammed earth built stock from Portugal is mainly concentrated in the southern region of the country, namely in Alentejo, Algarve and Ribatejo. However, it appears more often in southern Alentejo, where there is less rain and other building materials such as stone and timber [10]. In general, the Portuguese rammed earth built stock is classified according to its use, as civil and military. The fist group includes most of the built stock and is associated to the construction of dwellings, windmills, silos and religious constructions. The second group is mainly constituted by fortifications built during the Islamic presence in the Iberian Peninsula, between the 8th and 13th centuries [11].

Rammed earth, like other earthen materials, is considered as a non-industrial material [5], whose respective constructions usually show great vulnerability against several damaging agents, such as floods and earthquakes [1, 6]. The poor seismic performance of rammed earth constructions is due to several factors [7], from which the high dead-weight of these constructions, the very low tensile and shear strengths of the earthen materials and the poor connections between structural elements are the first to be evidenced. Therefore, two main types of failure mechanisms are expected from rammed earth walls under a seismic event with moderate to high intensity, namely out-of-plane collapse and in-plane shear failure [8]. Nevertheless, little is known about these mechanisms with regard to rammed earth, due to very limited research on this topic.

Unfortunately, a significant part of the rammed earth built heritage from Alentejo presents relative risk of loss or may put at risk the life of their inhabitants. The moderate seismic hazard of the region and the high seismic vulnerability of these constructions are key factors contributing for these risks. Furthermore, the seismic vulnerability of these constructions is worsened by the fact that many of them present an advanced level of structural decay or, in the worst scenario regarding their loss risk, are found abandoned. With respect to structural damage in rammed earth walls, two main forms can be referred, namely basal erosion and cracking (see Figure 2). The repair of these types of damage is essential to recover the initial structural performance of rammed earth constructions. However, their successful repair requires employing adequate intervention techniques, where the general compatibility between the parent material and the repairing one must be respected.

Basal erosion in rammed earth walls results in the reduction of the bearing section, which may lead to failure due to excessive compression stresses or, most probably, in overturning of the wall. This type of damage results from the long-term exposure of the walls to rainfall impact, wind erosion and biological activity. The repair of this type damage involves refilling the lost volume of material. A

simple technique to accomplish this involves compacting in place a mixture of a soil similar to that of the rammed earth wall, resorting to single-sided formwork. Steel reinforcements and plastic meshes are often included to promote the adhesion between the parent material and the repairing one. An alternative to this procedure, which mitigates possible shrinkage problems, consists in prefabricating earth blocks that are put in place and then bonded with earth mortar. The refilling with other materials, such as bricks, adobes and concrete are also reported in the bibliography [6, 13]. The projecting of earth is another possible repair technique, recently used in the in the conservation of Paderne Castle (Algarve, Portugal) [13] and in the Alhambra of Granada (Spain) [14].

(a) (b)

Figure 2. Structural damage in earth constructions [15]: (a) basal erosion; (b) cracking.

The presence of structural cracks in rammed earth walls decreases their bearing capacity and stiffness, and disrupts the overall monolithic behaviour of the structure. Furthermore, cracks constitute preferential paths for further decay caused by rainfall infiltration. In this case, the water can more easily access to the material inside the wall, decreasing substantially its mechanical properties. The formation of structural cracks in rammed earth walls is normally associated to settlements of the foundations, to concentrated loads, to horizontal thrusts applied by the roofs or to earthquakes. Several techniques are used to repair these cracks, but whose efficiency greatly varies from case to case. The most basic technique used to repair structural cracks consists in simply filling them with earth mortar. However, this technique fails in establishing the continuity and in the case where the crack is thin (less than ~30 mm), the wall needs to be cut back. Stitching the crack is another possible solution and consists in creating a mechanical connection between the two sides of the crack ("stapling" the crack). According to Keefe [16], this is carried out by cutting horizontal chases in the wall with a specific spacing along the crack, which are then filled with mud bricks and earth mortar prepared with a soil similar to that of the original rammed earth. Another technique being evidenced and studied in the last years is the grout injection [17]. In this case, the requirement for compatibility between materials has lead to the adoption of grouts incorporating earth, termed as mud grouts.

This paper presents an experimental program, where the shear behaviour of unstabilised rammed earth (URE) and the effectiveness of the injection of mud grouts in the repair of cracks are assessed. The URE from Alentejo was selected as a case study in order to contribute for developing the knowledge on these constructions, especially with respect to their performance under shear loading. This involved testing eleven URE wallets under diagonal compression. The tested specimens were reused to assess the repair effectiveness of two unmodified mud grouts (without the addition of current binders, such as cement, lime or gypsum) incorporating different percentages of the same soil used to manufacture the specimens.

2 EXPERIMENTAL PROGRAM

The experimental program involved the testing of eleven URE wallets under diagonal compression loading. These specimens were manufactured using a soil collected from Alentejo, whose suitability for URE construction was assessed in advance. The particle size distribution (PSD) of the soil required correction, which was performed according to recommendations for URE constructions. The

performance of the corrected soil was then assessed, in terms of compressive behaviour. These steps are described in the following sections, as well as the manufacturing and testing procedures of the URE wallets.

2.1. Soil characterization and URE suitability

The soil was collected in Amoreiras-Gare, Odemira (Alentejo), and was characterized by means of expeditious (sedimentation test, ribbon test, drop test and dry strength test) and laboratory (PSD analysis, Atterberg limits and standard Proctor) tests. Furthermore, the suitability of the soil for URE construction was assessed with basis on these tests (see [18] for more details).

In general, the expeditious tests revealed that the clay content of the soil was excessively high for being considering suitable for URE construction. This was confirmed by the PSD curve of the soil obtained by means of sieving a sedimentation analysis [19]. This curve is depicted in Figure 3 and compared against the PSD envelopes recommended by Houben and Guillaud [1] and by the Portuguese National Laboratory of Civil Engineering [20]. In both cases, the clay content of the soil (about 28%) is shown to be excessively high for URE.

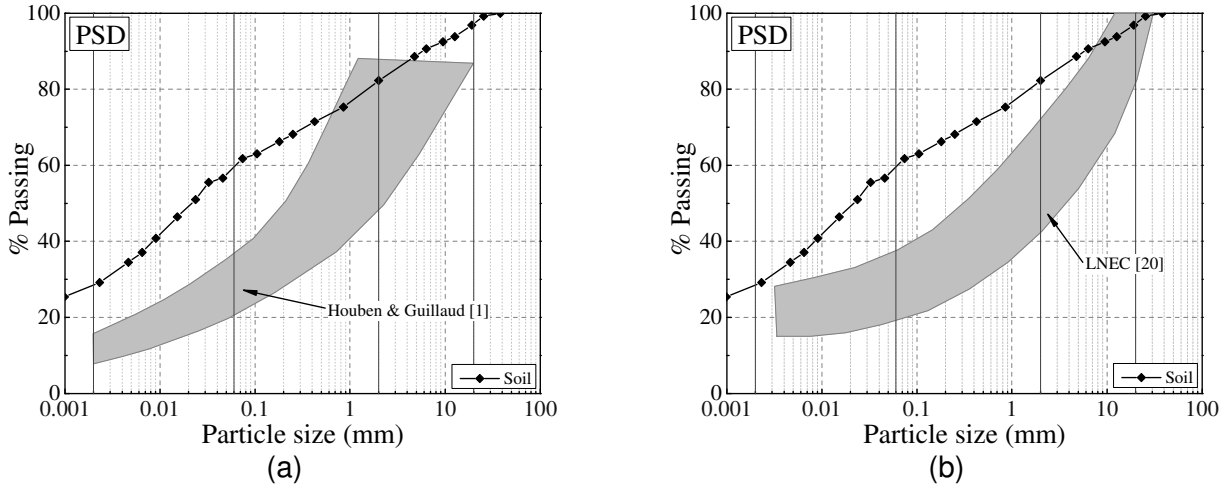

Figure 3. Comparison between the PSD curves of the soil and the envelopes for rammed earth construction recommended by: Houben and Guillaud [1]; (b); Portuguese National Laboratory of Civil Engineering [20].

The liquid limit (LL), plastic limit (PL) and shrinkage limit (SL) [21], as well as the plastic index (PI), shrinkage index (SI) and respective USCS classification of the soil are given in Table 1.

Table 1. Atterberg's limits and USCS classification of the soil.

LL (%)	PL (%)	PI (%)	SL (%)	SI (%)	USCS classification
30	18	12	22	8	Sandy lean clay (CL)

The results of the standard Proctor test [22] showed that the maximum dry density (ρ_{dmax}) of the soil was of about 1.83 g/cm^3 and the optimum water content (OWC) of about 13.4%. The value obtained for ρ_{dmax} is low for the case of rammed earth, which may mean that the correspondent mechanical performance may be insufficient.

In general, the characterization of the soil showed that it is unsuitable for URE. Its high clay content is the main reason leading to this conclusion, meaning that this soil needs PSD correction in order to be used in the manufacturing of the URE wallets.

2.2. Soil PSD correction

The PSD correction of the soil was carried out by means of the addition of river sand and gravel obtained from crushed granite. The PSD curves of these two aggregates are given in Figure 4, as well as the PSD of the corrected soil. The PSD correction consisted in adjusting the corrected PSD curve to the Fuller curve of Equation (1) [1], which allows optimizing the density of the respective URE and thus its mechanical performance.

$$P = \left(\frac{d}{D}\right)^{0.25} \quad (1)$$

where P is the percentage finer than the size being considered, d is the size being considered and D is the maximum size of the particles, which was assumed to be 19.1 mm.

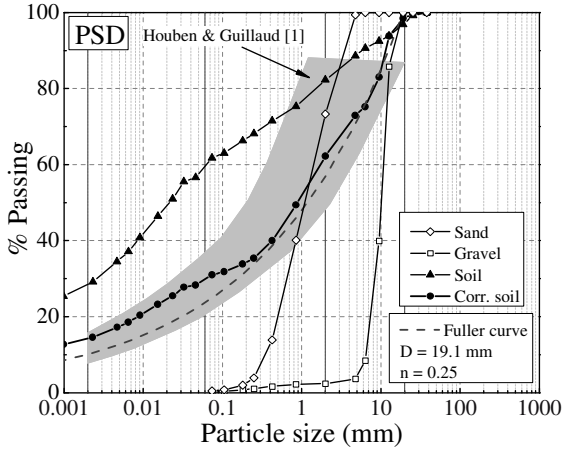

Figure 4. PSD correction of the soil.

The corrected soil was composed by 50% of the original soil, 28% of river sand and 22% of gravel (in weight). The properties of the corrected soil are given in Table 2. It should be noted that the initial clay content of the soil was reduced from 28% to 14%.

Table 2. Consistency limits and compaction properties of the corrected soil.

LL (%)	PL (%)	PI (%)	ρ_{dmax} (g/cm^3)	OWC (%)
23	16	7	2.10	10.1

2.3. Mechanical performance in compression

The compressive behaviour of the URE manufactured with the corrected soil was assessed by means of compression tests on six cylindrical specimens compacted with ρ_{dmax} and OWC. The specimens were compacted in three layers inside a metallic mould with dimensions of 100 mm diameter and 200 mm height. An electric rammer was used for this process and the specimens were demolded immediately after their compaction**.** The tests were carried out after the specimens achieving equilibrium water content at 20ºC temperature and 57.5% relative humidity (drying period between 27 and 35 days), which was found to be in average 1.04%. The vertical deformations at the middle third of each specimen were measured by means of three LVDTs radially-disposed to allow computing the Young's modulus. The load was applied in displacement control at a rate of 3 μm/s. In the day before testing, specimens had their top and bottom capped by a layer of gypsum. The stress-strain curves of the specimens, and the respective envelope, are presented in Figure 5. The compressive strength (f_c) of the specimens was of about 1.26 N/mm^2, being the least value of about 1.20 N/mm^2. This means that the compressive strength obtained deems with the minimum requirements of NZS 4298 [23], where the least value of a set of specimens must be higher than 1.14 N/mm^2 (after considering the

aspect ratio of the specimens). The average Young's modulus (E_0), computed between 5% and 30% of the respective f_c by linear fitting, was of about 1034 N/mm^2.

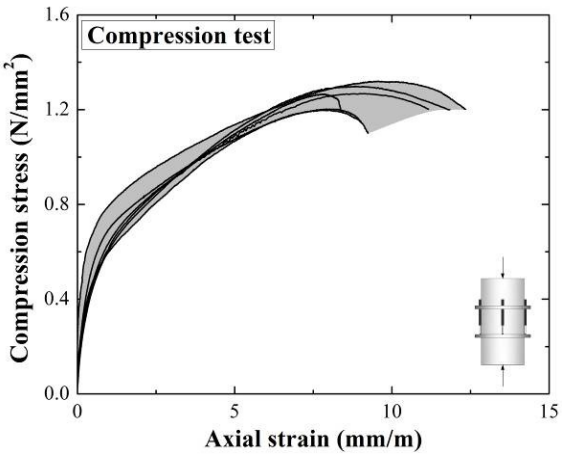

Figure 5. Stress-strain curves of the URE cylindrical specimens.

2.4. Manufacturing of the URE wallets

A total of eleven URE wallets were built with dimensions 550x550x200 mm^3 by compacting nine layers of moist earth within a high density plywood formwork (see Figure 6). The water content of the corrected soil for initiating the compaction was controlled by means of the drop test and all the specimens were demoulded immediately after compaction. The compaction was carried out by means of an electrical rammer. The wet weight and thickness of each layer was controlled during the compaction process in order to minimize the differences in density between specimens. The URE wallets were left to dry during 12 weeks at a room temperature of about 22±2ºC.

(a) (b) (c)

Figure 6. Manufacturing of the wallet specimens: (a) plywood formwork; (b) compaction with an electric rammer; (c) demoulding.

2.5. Testing procedure

The diagonal compression tests of the wallets were carried out after their drying and according to the procedure of ASTM E 519 [24]. The test setup is depicted in Figure 7. The supports were made of steel, with a width of about 100 mm, and the contact with the specimens was rectified by means of neoprene rubbers introduced between specimens and supports. The load was applied under monotonic displacement control at a rate of 2 μm/s and the vertical and horizontal displacements were measured in both faces of the wallets, resorting to LVDTs attached to the middle third of each diagonal. The same testing procedure was followed for the wallets after repairing by grout injection.

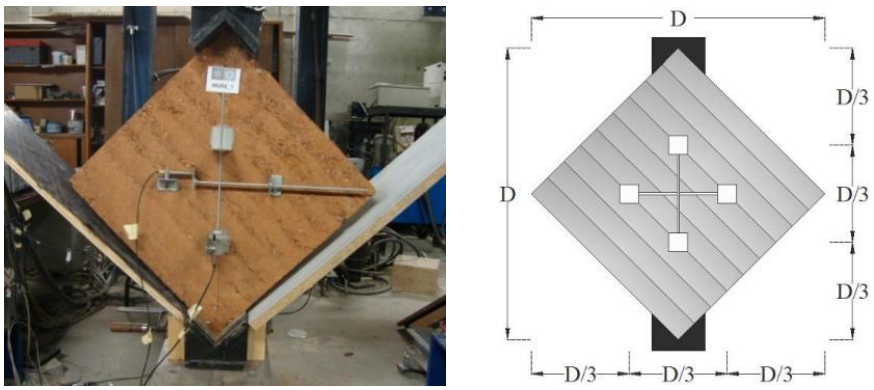

Figure 7. Test setup of the diagonal compression tests carried out on the URE wallets.

3 REPAIR OF THE SPECIMENS

The failure of the wallets divided them in some parts, which were removed from the testing apparatus and remounted together on a plywood board. Loose debris were removed from the failure surfaces before remounting the wallets. The assembling was carried out with the aid of an earth mortar prepared from the original soil used in the construction, but previously sieved to remove the particles larger than 4.75 mm. The remounting was performed by assembling piece by piece like building masonry, and when a specimen presented an high instability, it was tied by means of two plywood boards (Figure 8a). The aforementioned mortar was also used to seal the cracks on the surfaces of the specimens. Flexible plastic tubes with 6 mm diameter were installed in one of the sides of the specimens. The injection tubes were installed first in the intersection of cracks and then along the cracks, in such way that the spacing between injection tubes would be less than 100 mm. In the case of horizontal cracks, additional injection tubes were installed in the other side of the wallets in order to merely facilitate the air evacuation, whereby they were not used for injection.

(a) (b) (c)

Figure 8. Repair of the wallets by grout injection: (a) remounting of a wallet; (b) grout mixing; (c) injection of the grout.

Two unmodified mud grouts were used to repair the wallets, namely UMG40-60 and UMG50-50. Both grouts incorporated sieved soil (S#80) and limestone powder (200-OU) as solid phases, but the second grout incorporated a higher percentage of sieved soil. The sieved soil consisted of the original soil used in the construction of the specimens, but sieved in order to remove the particles larger than 0.180 mm. The limestone powder was obtained from a local supplier. Moreover, sodium hexametaphosphate (HMP) was used to improve the fluidity. The compositions and properties of both grouts are summarised in Table 3 and the respective PSD curves are plotted in Figure 9. It should be noted that the clay percentage of grout UMG40-60 is of about 21% and that of grout UMG40-60 is of about 25%. The higher clay content of grout UMG50-50 had very low impact on the fluidity (flow time) relative to grout UMG40-60, but the bending (f_b) and compressive (f_c) strengths improved significantly.

Table 3. Composition and properties of the mud grouts used in the repair of the URE wallets.

Grout	S#80 (wt.%)	200-OU (wt.%)	HMP (wt.%)	W/S	Flow time (s)	f_b (N/mm^2)	f_c (N/mm^2)
UMG40-60	40	60	0.46	0.30	36.5	0.92	2.44
UMG50-50	50	50	0.55	0.30	37.0	1.15	3.44

The preparation of each grout mixture required first weighing the solid components in order to prepare a grout volume of about 5 dm^3. The HMP was dissolved in the water necessary to prepare the grout, which was then added to the solid components. This blend was first hand-mixed (with a trowel) just to allow the water involving the solid components, and then was mixed with an electrical hand-mixer at maximum rotation speed (about 700 rpm) during 5 minutes (Figure 8b). The grouts were then sieved through ASTM sieve #10 (aperture size of about 2 mm) to remove agglomerates of particles.

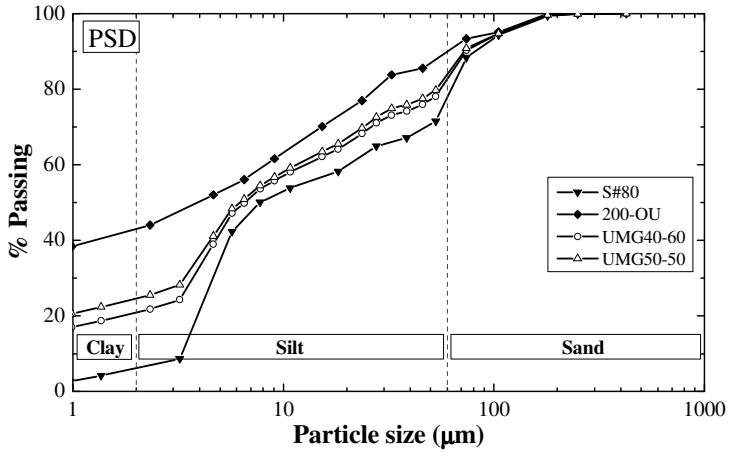

Figure 9. PSD of the composition materials and of the mud grouts.

Before injecting the wallets with the mud grout, 100 ml of water were injected in each injection tube, using a 100 ml capacity syringe. This procedure intended to mitigate the water sorption by the wallets and to check if the injection tubes were active. The wallets were injected with the mud grouts one hour after injecting the water, using the aforementioned 100 ml syringe (Figure 8c). The injection started by the lowest tube up to the top of the wallet. The tube being injected was sealed once the grout leaked from the next injection tube (normally the one immediately above). The injection was then carried out from the leaking tube, and so on. The occurrence of leakage from the sealing mortar was not very frequent and was easily solved by pressing soft paper against the leaking crack. Five wallets were repaired with grout UMG40-60 and six with grout UMG50-50.

4 RESULTS AND DISCUSSION

Table 4 and Table 5 summarize the results of the diagonal compression tests carried out on the wallets repaired with grout UMG40-60 and UMG50-50, respectively. These include the dry density (ρ_d), shear strength (f_{si}) and shear modulus (G_{0i}) before injection, shear strength (f_{sg}) and shear modulus (G_{0g}) after injection, shear strength recovery rate (f_{sg}/f_{si}) and shear modulus recovery rate (G_{gi}/G_{0i}). The shear moduli were computed between 5% and 30% of the shear strength of the respective specimen.

The average shear strength before injection in both sets of wallets was of about 0.15 N/mm^2, but this parameter presents some variability despite the low variability of ρ_d. Furthermore, the average value reported by Lacouture et al. [7] for URE (about 0.04 N/mm^2) is considerable lower than that reported

in this experimental program. It should be noted that the compressive strength reported by Lacouture et al. [7] was also considerably lower (0.55 N/mm^2). The obtained average shear strength here reported for URE is also significantly higher than that reported by Lacouture et al. [7] and Varum et al. [25] for adobe masonry (between 0.02 N/mm^2 and 0.03 N/mm^2). This low performance of adobe masonry can be explained by the fact that the mortar joints constitute a preferential failure surface.

Table 4. Results of the diagonal compression tests carried on the specimens repaired with grout UMG40-60 (coefficient of variation given inside brackets).

Specimen	ρ_d (g/cm^3)	f_{si} (N/mm^2)	f_{sg} (N/mm^2)	f_{sg}/f_{si} (%)	G_{0i} (N/mm^2)	G_{gi} (N/mm^2)	G_{gi}/G_{0i} (%)
WURE_1	2.02	0.17	0.07	39	659	67	10
WURE_2	2.06	0.16	0.15	93	705	53	8
WURE_3	2.04	0.13	0.06	43	413	47	11
WURE_4	2.03	0.14	0.09	68	341	54	16
WURE_11	2.04	0.14	0.12	89	732	142	19
Average	2.04 (1%)	0.15 (10%)	0.10 (40%)	66 (38%)	570 (32%)	73 (54%)	13 (37%)

Table 5. Results of the diagonal compression tests carried on the specimens repaired with grout UMG50-50 (coefficient of variation given inside brackets).

Specimen	ρ_d (g/cm^3)	f_{si} (N/mm^2)	f_{sg} (N/mm^2)	f_{sg}/f_{si} (%)	G_{0i} (N/mm^2)	G_{gi} (N/mm^2)	G_{gi}/G_{0i} (%)
WURE_5	2.01	0.11	0.09	77	464	89	19
WURE_6	1.97	0.14	0.07	52	646	33	5
WURE_7	2.02	0.17	0.09	55	640	29	5
WURE_8	2.03	0.13	0.09	68	1036	73	7
WURE_9	2.02	0.14	0.07	54	807	66	8
WURE_10	2.04	0.19	0.09	46	661	45	7
Average	2.01 (1%)	0.15 (19%)	0.08 (10%)	59 (20%)	709 (27%)	56 (43%)	8 (64%)

The average shear strength of the wallets after being repaired by injection is of about 0.10 N/mm^2 and 0.08 N/mm^2 for the case of the set of wallets repaired with grout UMG40-60 and that repaired with grout UMG50-50, respectively. This corresponds to an average shear strength recovery rate of about 66% and 59%, respectively. These values are somehow far from the complete shear strength recovery (100%), which in practice is a goal hardly achieved. The wallets are expected to present damage at the micro level (ex: micro-cracking), which is not possible to be repaired by injection. Despite that, both grouts presented a satisfactory performance regarding the adhesion capacity. Another important observation to be highlighted is that the grout UMG50-50 promoted a recovery rate slightly lower than grout UMG40-60, despite its higher strength. In fact, the performance of both grouts is similar, indicating that higher clay percentage may not mean a higher adhesion capacity and that the repair capacity may have been limited by the damage introduced during the first test.

The shear stress-strain curves of the wallets before and after injection are presented in Figure 10. With respect to the behaviour of both sets of wallets before repair, it is observed that most of the wallets present an early peak shear stress, after which the shear strain has a fast increase. This early peak shear stress is thought to be related to cohesion (i.e. to the binding capacity) promoted by the clay fraction. In fact, the shear behaviour of the wallets up to this peak stress results from the contribution of the clay fraction cohesion, and friction and interlocking capacity of the coarse aggregates. After this point, the contribution of the cohesion is lost and the shear behaviour of the wallets relies only on the friction and interlocking. Moreover, some wallets present a hardening behaviour after this stress, which can be explained by a superior interlocking occurring in these wallets. Another important contribution of the friction and interlocking to the shear behaviour of the wallets is that all wallets (with exception of WURE_4) present large shear deformation capacity, and thus ductility. This is an important feature for rammed earth in the case of a seismic event, which is expected to contribute for the energy dissipation.

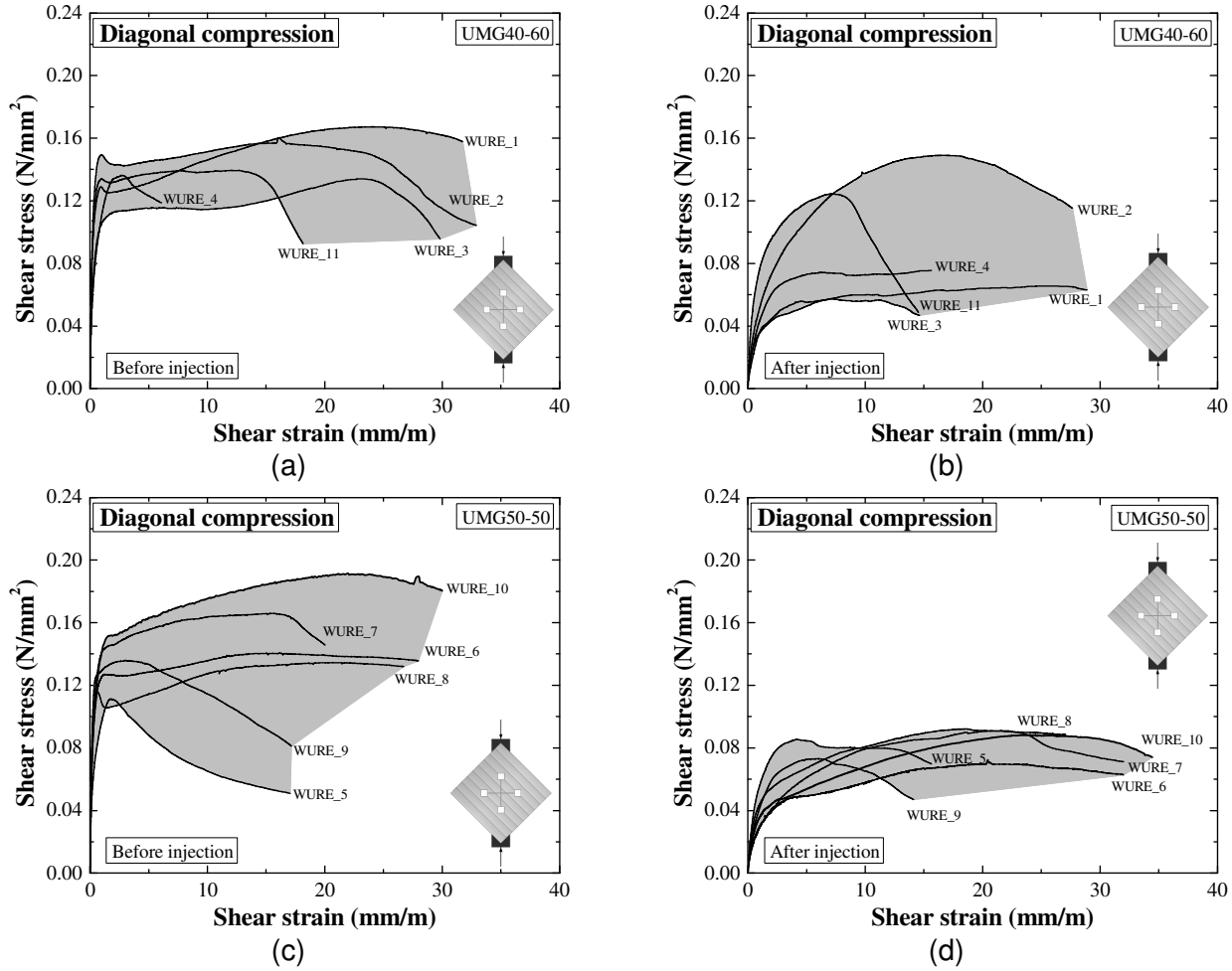

Figure 10. Shear stress-strain curves of the wallets: (a) set repaired with grout UMG40-60 before injection; (b) set repaired with grout UMG40-60 after injection; (c) set repaired with grout UMG50-50 before injection; (d) set repaired with grout UMG50-50 before injection.

With respect to the shear stress-strain curves of the wallets after injection, it is observed a substantial decrease in stiffness relative to the performance before injection, no matter the grout used. The average G_{0g} corresponds to an overall decrease of about one order of magnitude with respect to G_{0i}. This important decrease may be explained by less efficient interlocking and friction mechanisms in the wallets after repair. In fact, the interlocking at the failure surface in the first test of the wallets was provided by coarse aggregates, which were then lost in the reassembling of the specimens and not reintroduced by the injection. Therefore, this potential failure surface was smoothed by the first test

reducing the friction of what is an obvious preferential failure surface for the second test. Moreover, the lower interlocking and friction of the repaired wallets can also be pointed out as a reason to explain a shear strength recovery that was shown to be relatively inferior to the total recovery.

The failure of the wallets before injection occurred as a consequence of the formation of a main crack or set of cracks with predominant diagonal orientation, crossing the entire specimen (Figure 11a). The formation of these cracks or set of cracks was observed visually to start before the peak load, at the middle of the specimens, and then developed toward the top and bottom supports. In general, the crack pattern of the wallets after injection followed that before injection, confirming that the initial cracks constitute preferential surfaces for failure (Figure 11b).

(a) (b)

Figure 11. Failure mode of wallet WURE_4: (a) before injection; (b) after injection.

5 CONCLUSIONS

The experimental program presented in this paper addressed the shear behaviour of URE before and after the repair with injected unmodified mud grouts. In general, the shear behaviour of URE was shown to result from the contribution of the binding promoted by the clay fraction of the soil and of the friction and interlocking promoted by the coarse aggregates. The friction and interlocking was also shown to control the non-linear behaviour of URE and to promote a significant deformation capacity.

With respect to the injection repair, both grouts used presented a satisfactory and similar recovery capacity of the shear strength. This also showed that no advantage was gained from using a stronger unmodified mud grout. Nevertheless, this repair technique was shown to be incapable of recovering completely the initial shear strength of URE specimens due to its incapacity for repairing micro-level damage. Furthermore, the injection technique was shown to be incapable of re-establishing the initial shear stiffness of the specimens, which is a result from the incapacity of the mud grout in recovering the interlocking promoted by the coarse aggregates at the cracks.

ACKNOWLEDGEMENTS

The financial support provided by the Portuguese Science and Technology Foundation through the project FCOMP-01-0124-FEDER-028864 (FCT-PTDC/ECM-EST/2396/2012) is gratefully acknowledged.

REFERENCES

[1] Houben, H. & Guillaud, H.: *Earth Construction: A Comprehensive Guide*, CRATerre – EAG, Intermediate Technology Publication, London 2008.

[2] Minke, G.: *Building with earth: Design and technology of a sustainable architecture,* Birkhäuse-Publishers for Architecture, Basel-Berlin-Boston 2006.

[3] Jaquin, P.A.: One third of world's population live in earth buildings? http://historicrammedearth.com/one-third-of-worlds-population-live-in-earth-buildings, 2013.

[4] Jaquin, P.A.; Augarde, C.E. & Gerrard, C.M.: A chronological description of the spatial development of rammed earth techniques. International Journal of Architectural Heritage, 2 (2008), 377-400.

[5] Bui, Q.B.; Morel, J.C.; Hans, S. & Meunier, N.: Compression behaviour of non-industrial materials in civil engineering by three scale experiments: the case of rammed earth. Materials and Structures, 42 (2009), 1101-1116.

[6] Warren, J.: *Conservation of Earth Structures*, Butterworth Heinemann, Bath 1999.

[7] Lacouture, L.; Bernal, C.; Ortiz, J. & Valencia, D.: *Studies on seismic vulnerability, rehabilitation and strengthening of adobe and rammed earth houses*, Apuntes 2007, 20 (2): 286-303. (in Spanish)

[8] Oliveira, D.V.; Silva, R.A.; Lourenço, P.B. & Schueremans, L.: *Rammed earth constructions and the earthquakes*. In: Proc. of the Congresso Nacional de Sismologia e Engenharia – SÍSMICA 2010, eds. A. Costa, C.S. Oliveira & H. Varum, Aveiro 2010, 1-13. (in Portuguese)

[9] Correia, M.: *Rammed Earth in Alentejo*. Argumentum: Lisbon 2007.

[10] Rocha, M.: Rammed *earth in traditional architecture: construction techniques*. In: Earth architecture in Portugal (2005), Argumentum: Lisbon, 22-26.

[11] Correia, M. *Islamic fortresses in military rammed earth*, Pedra & Cal, 24 (2004), 16. (in Portuguese)

[12] Mileto, C.; Vegas, F. & López, J.M.: *Criteria and Intervention Techniques in Rammed Earth Structures. The Restoration of Bofilla Tower at Bétera*. Informes de la Construcción, 63 (2011), 81-96.

[13] Cóias, V. & Costa, J.P.: *Terra Projectada: Um Novo Método de Reabilitação de Construções em Taipa.* In: Houses and Cities Built with Earth: Conservation, Significance and Urban Quality, eds. M. Achenza, M. Correia, M. Cadinu & A. Serra, Argumentum: Linbon 2006, 59-61.

[14] García, R.M. *Construcciones de Tierra. El Tapial. Nuevo Sistema para Construcción y Restauración Mediante la Técnica de "Tierra Proyectada"*, PhD thesis, University of Granada, Granada 2010.

[15] Silva, R.A.; Jaquin, P.; Oliveira, D.V.; Miranda, T.; Schueremans, L. & Cristelo, N.: Conservation and new construction solutions in rammed earth. In: Structural Rehabilitation of Ancient Buildings, eds. A. Costa; J. Miranda; H. Varum, Springer-Verlag: Berlin 2014, 77-108.

[16] Keefe, L.: *Earth Building: Methods and materials, repair and conservation*, Taylor & Francis: London 2005.

[17] Silva, R.A.; Schueremans, L.; Oliveira, D.V.; Dekoning, K. & Gyssels, T.: *On the development of unmodified mud grouts for repairing earth constructions: rheology, strength and adhesion*. Materials and Structures 2012, 45(10), 1497-1512.

[18] Silva, R.A.: Repair of earth constructions by means of grout injection. PhD thesis, University of Minho / KUleuven. 2013.

[19] LNEC E196: Solos: Análise granulométrica. Laboratório Nacional de Engenharia Civil: Lisbon. 1966.

[20] LNEC. The use of earth as a building material. Laboratório Nacional de Engenharia Civil: Lisbon. 1953. (in Portuguese)

[21] NP 143: Soils: determination of the consistency limits. Laboratório Nacional de Engenharia Civil: Lisbon. 1969. (in Portuguese)

[22] LNEC E197: Compaction test. Laboratório Nacional de Engenharia Civil: Lisbon. 1967. (in Portuguese)

[23] NZS 4298: Materials and workmanship for earth buildings. Standards New Zealand: Wellington. 1998.

[24] ASTM E 519: Standard Test Method for Diagonal Tension (Shear) in Masonry Assemblages. American Society for Testing and Materials: West Conshohocken. 2002.

[25] Varum, H.; Silveira, D.; Carvalho, J.; Figueiredo, A. & Costa, A. (2011) Characterization of the mechanical behaviour of adobe masonry walls. In: Proc. of Construcción com tierra. Tecnologia y Arquitectura. Congresso de tierra en Cuenca de Campos, Valladolid 2011, 225-228.